Available online at www.sciencedirect.com
ScienceDirect
International Journal of Heat and Mass Transfer 51 (2008) 1933–1945
International Journal of HEAT and MASS TRANSFER
www.elsevier.com/locate/ijhmt

Inverse radiation problem to retrieve hydrometeors from satellite microwave radiances

V. Swaminathan [a,b], R.M. Gairola [a,c], C. Balaji [a,*], V.K. Agarwal [a,c], S.P. Venkateshan [a]

[a] *Heat Transfer and Thermal Power Laboratory, Department of Mechanical Engineering, Indian Institute of Technology Madras, Chennai 600 036, India*
[b] *Thermal Specialist, Flomerics India Pvt. Ltd., 581/2, 8th Block, Koramangala, Bangalore 560 034, India*
[c] *Scientist, Oceanic Sciences Division, Remote Sensing Applications Area, Space Applications Centre (ISRO), Ahmedabad 380 015, India*

Received 5 April 2006; received in revised form 24 May 2007
Available online 18 September 2007

Abstract

This study presents a new hybrid method that combines regression analysis with genetic algorithms for the retrieval of hydrometeors (cloud liquid water, ice and rain) in the atmosphere, from satellite microwave radiances. A three layered atmosphere model (divided into 30 sub-layers) is used to generate simulated profiles of hydrometeors. The equation governing the transfer of radiation is solved using the finite volume method to obtain radiances (brightness temperatures) in the microwave region. This is known as the forward problem and is solved repeatedly to create a database with which regression equations are developed for the monochromatic microwave radiances, for six typical frequencies ranging from 6.6 to 85 GHz. The regression is done using nonlinear parameter estimation techniques. The inverse problem of retrieving the hydrometeors characteristics from microwave radiances is accomplished by posing the parameter estimation problem as an optimization problem, wherein, minimization of the sum of squares of residuals between the estimated and known radiances, for the above mentioned six typical frequencies, is done. In this study, genetic algorithms have been used for solving the minimization problem.

Keywords: Radiative transfer; Atmosphere; Retrieval; Finite volume method; Genetic algorithms; Hydrometeors; Microwave frequencies; Regression equations

1. Introduction

Precipitation (any form of water that falls on to the earth's surface) is an important part of the global energy cycle, since moisture is an important channel of atmospheric heat transport. The uneven heating of the earth creates areas of warm air that tend to rise. When the warm air rises, it leaves behind a gap that's filled by air from surrounding regions moving in. As the warm air rises it expands and cools. Since cool air cannot hold as much moisture, this often results in precipitation (called convective precipitation). Quantitative assessment of precipitation is needed to improve the understanding of the behaviour of global energy and circulation patterns. Since 70% of the earth is covered with water, land-based techniques of rainfall estimation (for example, raingauges) are not sufficient for global rainfall estimation. Hence, one uses satellite remote sensing of clouds and precipitation for global estimation of rainfall. In the remote sensing scenario, an orbiting satellite records radiant energy at wavelengths that range from the visible, infrared to the microwave regime. Various algorithms can then be used to estimate rates of rainfall from the emergent radiant energies.

Compared to visible and infrared observations, satellite remote sensing using microwave data is a new development and provides more accurate, instantaneous retrievals, due to the direct physical relationship between microwave radiation and column cloud, rain water and ice. Many microwave rainfall retrieval algorithms have been developed in

* Corresponding author. Tel.: +91 44 22574689.
E-mail address: balaji@iitm.ac.in (C. Balaji).

0017-9310/$ - see front matter © 2007 Elsevier Ltd. All rights reserved.
doi:10.1016/j.ijheatmasstransfer.2007.06.030

Nomenclature

Avg_CLW average of cumulative cloud liquid water content, g m^{-3}
Avg_Ice average of cumulative ice content, mm/h
Avg_Rain average of cumulative rain content, mm/h
BT brightness temperature, K
C_{lw} normalized average of cumulative cloud liquid water content (refer Table 3)
C_1 first Rayleigh–Jeans constant, 0.59552197×10^8 Wμm^4 m^{-2} s r^{-1}
C_2 second Rayleigh–Jeans constant, 14387.69 μm K
F,f objective function
g asymmetry factor or function defined in Eq. (4)
I radiation intensity, W m^{-2} s r^{-1}
$\bar{I}$ in-scattering term, W m^{-2} s r^{-1}
I_{ce} normalized average of cumulative ice content (refer Table 3)
J Jacobian
p parameter vector defined in Eq. (7)
q correction to the parameter vector defined in Eq. (10)
Rain1 rainfall rate in 1st layer, mm/h
Rain2 rainfall rate in 2nd layer, mm/h
R_C normalized average of cumulative rainfall rate (refer Table 3)
R_1, R_2 normalized rainfall rate in 1st and 2nd layer, respectively (refer Table 3)
s coordinate along ray path, m
S residual defined in Eq. (5)
T absolute temperature, K
T_B normalized brightness temperature (refer Table 3)
T_B^* normalized, known brightness temperature (refer Table 3)
$X_1 \ldots X_4$ dummy variables used in GA (refer Appendix A)
z coordinate along vertical direction, m

Greek symbols
ε emissivity of surface or damping factor defined in Eq. (11)
ϕ azimuthal angle, rad
Φ scattering phase function
γ polar angle, rad
κ absorption coefficient, m^{-1}
λ wavelength, μm
ν frequency, GHz
σ_s scattering coefficient, m^{-1}
ω solid angle, sr
ρ correlation coefficient

Subscripts
actual already available data
b black body
correlation data obtained using correlation
retrieved retrieved using genetic algorithm
z z direction
λ, ν spectral quantity

Superscripts
L lower limit
T transpose of the matrix
U upper limit
′ incoming direction

the last two decades [1–3]. From the reviews, one can see that, retrieval of precipitation using passive microwave sensors is developing at a rapid pace, with a lot of effort going towards improving cloud models [4–7] and also retrieval algorithms [8–10]. Independently, considerable work is also going on in developing new methods to solve the equation of transfer with added complexities like polarization and anisotropic scattering.

The present work is concerned with retrieval of column rainfall rate, ice content and cloud liquid water simultaneously by using the signal (radiance/brightness temperature) emerging from the top of the atmosphere in the microwave regime. This signal is frequently referred to as the TOA (top of the atmosphere) radiance and is recorded by the passive remote sensing device. The signal results from the radiant energy which is emitted and scattered by the surface (either land or ocean), by the clouds, raindrops, ice and atmospheric gases (such as H_2O and O_2).

In this numerical study, the forward calculations are carried out with known atmospheric constituents to obtain the brightness temperatures. These will be treated as the satellite measured brightness temperature values for the inverse problem, in the place of real satellite measured brightness temperatures. The frequencies used for the forward calculations are $\nu_1 = 6.600$, $\nu_2 = 10.700$, $\nu_3 = 19.350$, $\nu_4 = 22.235$, $\nu_5 = 37.500$ and $\nu_6 = 85.000$ GHz, respectively. These are selected by noting that these frequencies are used in passive microwave radiometers such as the Electrically Scanning Microwave Radiometer (ESMR) aboard the Nimbus-5 satellite [11], the Scanning Multichannel Microwave Radiometer (SMMR) aboard the Nimbus-7 satellite [12], the Special Sensor Microwave/Imager (SSM/I) [13], the TRMM Microwave Imager (TMI) [14], the Advanced Microwave Scanning Radiometer for Earth Observing System (AMSR-E) [8]. AMSR-E is the instrument with a set of frequencies that most closely resembles that used in this paper.

From the review of the literature, one can see that, often, the procedure that has been used in the literature for the retrieval of parameters is to solve the direct problem

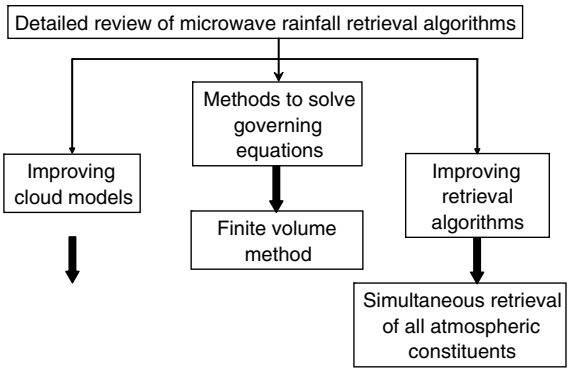

Fig. 1. A bird's eye view of current research vis-à-vis the approach proposed in the present study in respect of rainfall retrieval algorithms.

repeatedly to calculate the brightness temperatures for different microwave frequencies for a huge set of simulated profiles (or real profiles). By using the simulated profiles along with the direct problem results, inverse regression equations are developed that will estimate the parameters as a function of the brightness temperatures at different microwave frequencies. If one looks at the above procedure carefully, the number of parameters required to calculate the brightness temperature during the forward problem is large, but in the retrieval only one parameter is retrieved from the brightness temperatures at different microwave frequencies, without considering the effects of other parameters. In this study, an attempt is made to simultaneously retrieve all the parameters that are used in the calculation of brightness temperature in the forward problem. A new hybrid approach is proposed, in which the forward problem of determining the brightness temperature from the input profiles is carried out through regression analysis. The inverse problem to retrieve the cloud parameters is then solved as an optimization problem, utilizing genetic algorithms (GA). GA comes under the category of non-traditional optimization algorithms and is used extensively for problems involving multimodal functions [15–17].

A bird's eye view of the state-of-the-art in the area of rainfall retrieval vis-à-vis what we propose to undertake in this study is given in Fig. 1.

2. Physical model

This is a paper on methodology or, more explicitly, an exposition of a technique for generating retrieval algorithms. In view of this, the physical model for the precipitating atmosphere is intentionally kept simple. Even so, the important quantities of interest like column rainfall rate, ice and cloud liquid water content are present in the model.

The cloud model used in this study is a simple vertically structured, plane-parallel, horizontally infinite representation of a raining atmosphere similar to that of [18] and [19]. Fig. 2 depicts the one-dimensional geometry used for representing the atmosphere in this study. The bottom surface is considered to be having a wavelength averaged

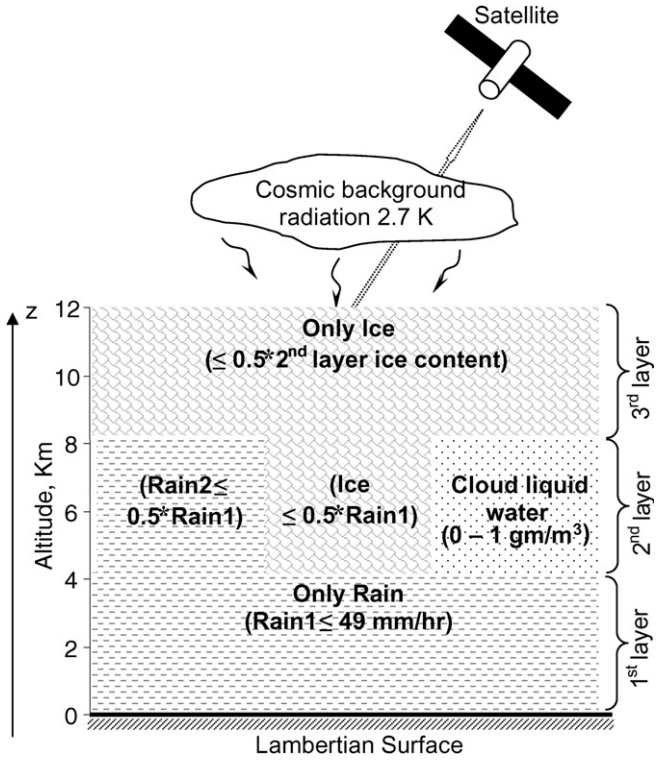

Fig. 2. A schematic illustration of passive microwave remote sensing with distribution and range of hydrometeors.

emissivity, ε. At the top of the atmosphere, cosmic background radiation at 2.7 K is assumed.

Vertical hydrometeor profiles (including raindrops, ice particles, and cloud liquid water) are specified from 0 to 12 km, with the atmosphere divided equally into three layers of height 4 km each. The distribution and range of hydrometeors within each layer is shown in Fig. 2. The rain rate is kept constant from the surface to 4 km. Between 4 and 8 km, the hydrometeors are kept constant and are assumed to be made up of rain, solid ice and cloud liquid water content. The hydrometeors from 8 to 12 km are assumed to be kept constant and made up of only solid ice content. The bottom surface emissivity, temperature and lapse rate are assumed to be 0.5, 288 K and 6.5 K/km, respectively. The relative humidity throughout the cloud is set constant at 90%. This study considers the effect of surface polarization (only vertical polarization) and atmospheric polarization is ignored. Vertical polarization is not affected by wind speeds for speeds less than 8 m/s, and this effectively removes wind speed as a parameter in the model. Since the focus of this paper is on the demonstration of the algorithm, the assumption of a uniform oceanic emissivity is not expected to severely constrain the physical model. Furthermore, oceanic emissivities are known to vary from 0.3 to 0.7 and so the median value also turns out to be 0.5. This value has also been used by other investigators (see, for example, Lin and Minnis [20]).

When the algorithm proposed in this study is to be applied to real data, these assumptions have to be relaxed and the cloud model will then be necessarily complex.

3. The forward problem

3.1. Mathematical model

The problem of concern is to numerically determine the TOA radiances/ brightness temperatures emerging out of the atmosphere that will have been recorded by the passive microwave remote sensing device, at a given instant of time at a given location on the ocean (or land). These will subsequently be used in the retrieval algorithm. The equation to be solved is the radiative transfer equation that describes the change in intensity over the path length s for a participating medium through which radiative energy travels and is given by [21]

$$\frac{\mathrm{d}I_\lambda}{\mathrm{d}s} = -(\kappa_\lambda + \sigma_{s\lambda})I_\lambda(s) + (\kappa_\lambda I_{b\lambda}(s) + \sigma_{s\lambda}\overline{I}_\lambda(s,\omega,\omega')) \quad (1)$$

The terms on the right-hand side of Eq. (1) represent the contributions from absorption, scattering away from the direction $\vec{s}$, emission, and scattering into the direction of $\vec{s}$. In the microwave region (large wavelength or small frequency), the Rayleigh–Jeans formula is used to represent the blackbody intensity and is given by

$$I_{b\lambda} = \frac{2C_1 T(z)}{C_2 \lambda^4} \quad (2)$$

Since the microwave radiant intensity or radiance is directly proportional to temperature, $T(z)$ is interpreted, and known, as the brightness temperature. The in-scattering term is given by

$$\overline{I_\lambda}(s,\omega,\omega') = \frac{1}{4\pi}\int_{\omega'=0}^{4\pi} I_\lambda(s,\omega')\Phi_\lambda(\omega,\omega')\mathrm{d}\omega' \quad (3)$$

The anisotropic scattering property of the particles in the atmosphere is approximated by retaining only a certain number of terms of the Legendre polynomial series expansion. In this study, a linear anisotropic scattering model is used, in which only the first two terms of the series are used. The phase function has the following mathematical representation [22].

$$\Phi(\lambda,\omega,\omega') = 1 + 3g(\lambda,z)(\cos\gamma'\cos\gamma + \sin\gamma'\sin\gamma\cos(\phi'-\phi)) \quad (4)$$

The details of the finite volume formulation of the governing time-independent radiative heat transfer equation and its method of solution are available in references like [23] and [24], and hence for brevity are not discussed here. The finite volume method is justified because it is demonstrably a superior algorithm [25,26] when heavy scattering is involved, as for example in a raining atmosphere, like the one considered in this study. The effect of the grid size on the solution is studied in a manner similar to that reported in [24] in order to fix the optimum number of control volumes and the number of directions. Accordingly, the number of directions was fixed at 20 and the number of control volumes within a layer was fixed at 10. The conversion of atmospheric constituents in each layer to its corresponding asymmetry factor, absorption and scattering coefficients was carried out using a program developed by Kummerow [27].

3.2. Results for the forward problem

Validation of the forward problem along with the results is documented in [25]. Even so, for the sake of completeness, we present some salient features of the results that will help us better understand the complexities that can be expected in the retrieval process. The variation of the brightness temperatures with respect to the cloud liquid water content was found to be weak compared to their variation with respect to rainfall rate and ice content. While at high frequencies, when the rainfall changes from 0 mm h to 49 mm h, the brightness temperature can be pulled down by as much as 200 K for a given ice content and cloud liquid water content, at high frequencies the effect of cloud liquid water content on the brightness temperature is almost negligible. The effect of ice content is in between and it becomes pronounced at higher frequencies. However, the effect of rain on the brightness temperatures is strong at all frequencies, including the lower ones (6.6 and 10. 7 GHz). For a no raining case, with negligible ice content, the presence of clouds can bring down the brightness temperatures only to the extent of about 30 K and this decrease tapers off at higher frequencies. *It is now intuitively apparent, that retrieval of cloud liquid water in a raining atmosphere will be very difficult*. We will return to this point in Section 5. The effects of various parameters are succinctly presented in Tables 1 and 2. While Table 1 gives the lower and upper bounds of the TOA satellite signal, i.e. the brightness temperatures for various frequencies, for the assumed physical model, Table 2 gives a qualitative idea of the effect of various parameters on the brightness temperatures for the six frequencies under consideration and can be called as a trend analysis.

The above findings can be concisely summarized as (1) emission is dominant at 6.6 and 10. GHz (2) scattering is dominant at 37.5 and 85 GHz and (3) both emission and scattering are significant at 19.35 and 22.235 GHz.

Table 1
Lower and upper bounds for TOA brightness temperatures for various frequencies

Frequency (GHz)	Range of TOA brightness temperatures (K)
6.600	150–240
10.700	150–270
19.350	100–270
22.235	120–270
37.500	70–270
85.000	50–260

Table 2
Trend analysis for the results of the forward model

Frequency (GHz)	What happens to brightness temperature With increase in rainfall rate	
	With no ice content	With increase in ice content
6.6	Increases	Increases
10.7	Increases	For low ice content – increases For high ice content – increases and then decreases
19.35	Increases and becomes constant	Increases and then decreases
22.235	Increases and becomes constant	Increases and then decreases
37.5	Increases and becomes constant	For low ice content – increases and then decreases For high ice content – decreases
85	Increases and becomes constant	Decreases

4. The inverse problem–hybrid method

The inverse problem refers to the full blown retrieval of all the parameters that affect the forward calculations. Stated more explicitly, *for a set of frequencies if the brightness temperatures are known or measured, one needs to determine the atmospheric constituents that led to those brightness temperatures.* In the parlance of optimization, this problem is referred to as a *parameter estimation problem*. While several techniques are available for estimation of parameters, the retrieval gets increasingly difficult when (1) the number of parameters becomes large and (2) there is complex interplay between the variables or the effects they cause. A highly reliable approach would be to pose the parameter estimation problem as an optimization problem wherein we minimize the "error" between the known brightness temperature values (referred to as measured values) and the calculated brightness temperature values corresponding to the frequencies under consideration. The "error" referred to above is in a least squares sense. Optimization algorithms that use the least square approach are known as LSR (least square residual) techniques. Typically, the first step in an LSR approach would be to calculate the dependent variable, in this case the brightness temperatures using the forward model, by assuming some guess values for the unknown parameters. Corresponding to the error between the known brightness temperature values with that of calculated brightness temperature values, by using some optimization algorithms, subsequently new values will be assigned to the unknown parameters until the error gets minimized to an acceptable value. The corresponding final values of the unknown parameters will give the corresponding atmospheric constituents which gave rise to the known brightness temperatures. In view of the highly complex nature of the problem under consideration, in this study, the optimization is carried using genetic algorithms (GA), a multidimensional search technique that mimics the process of evolution.

For the problem under consideration, since the forward calculations of brightness temperatures have to be carried out a number of times in order to obtain the final values of the unknown parameters for just one set of atmospheric profiles, in reality there will be a huge data set of brightness temperatures corresponding to number of different atmospheric profiles obtained through observations from remote sensing satellites. In view of this, it will become impossible to run through the forward calculations again and again, as this would involve a large amount of computer time. In order to speed up the retrieval algorithm, the procedure described below is used to develop relations between the brightness temperature and parameters of interest and these relations are used to calculate brightness temperatures instead of using forward calculations repeatedly. Here again, we take recourse to nonlinear parameter estimation techniques. *In effect, for both the forward and inverse calculations, we have employed optimization techniques in this study.*

Approximately, 21,000 profiles were "synthetically" generated by varying the hydrometeor content in each layer, within the range specified in Fig. 2, out of which 15,000 profiles were used to generate the regression equations and the remaining 6000 were used for validation purposes. Use of synthetically generated profiles offers an alternative to the use of field data and is frequently used in the evaluation of new retrieval algorithms. The main advantage of this approach is the ability to generate any number of profiles to be used for creating a database and this removes the difficulty posed by limited datasets obtained from field measurements (see [28] who discuss a numerical method for synthesizing atmospheric and humidity profiles).

The synthetically generated profiles were used, in conjunction with the finite volume method outlined in Section 3, to evaluate the TOA brightness temperatures, at a generic viewing angle of 50° (normal viewing angles vary from 50° to 55 °) for frequencies 6.6 GHz, 10.7 GHz, 19.35 GHz, 22.235 GHz, 37.5 GHz and 85 GHz.

4.1. Normalization

All the parameters involved in the current study are normalized with respect to their maximum possible values shown in Table 3. Normalization is carried out with a view to have smaller values for the coefficients in the regression equations and to ensure that the range of all variables gets fixed between 0 and 1. This also helps in reducing some effort needed to code the variable limits in the optimization analysis, which is used for solving inverse problem in the current study.

4.2. Forward calculations using regression analysis

Regression equations were developed using the generated data set, to obtain brightness temperature for each frequency in terms of cloud liquid water content, rainfall rate and ice content using the commercially available DATAFIT 8.1 [29]. Here again, the parameters in the regression equation are determined by minimizing the error between

Table 3
Normalization for various parameters

Parameters	Maximum value in 1st layer	Maximum value in 2nd layer	Maximum value in 3rd layer	Average of the maximum value for three layers	Normalization	Symbol
Brightness temperature	–	–	–	–	BT/288	T_B, T_B^*
Cloud liquid water	0	1.0	0	0.334	Avg_CLW/0.334	C_{lw}
Ice content	0	24.5	12.25	12.25	Avg_Ice/12.25	I_{ce}
Rainfall rate in 1st layer (mm/h)	49	–	–	49	Rain1/49	R_1
Rainfall rate in 2nd layer (mm/h)	–	24.5	–	24.5	Rain2/24.5	R_2
Cumulative rainfall rate (mm/h)	49	24.5	0	24.5	Avg_Rain/24.5	R_C

the sum of the squares of residuals between the regression model and the data using the Levenberg–Marquardt algorithm (LMA) with double precision. LMA is capable of solving nonlinear equations and returning the coefficients of the supplied regression model. In what follows, a brief discussion on the LMA is presented. The generalized problem of least squares minimization, concerning the brightness temperature for a particular frequency, can be stated as

$$S = \sum_{i=1}^{n} [T_B^* - T_B(R_1, R_2, C_{lw}, I_{ce})]^2 \tag{5}$$

Eq. (5) can be rewritten as

$$S(p) = \sum_{i=1}^{n} [g_i(p)]^2 \tag{6}$$

where p is the parameter vector given by

$$p^T = (R_1, R_2, C_{lw}, I_{ce}) \tag{7}$$

$$\text{and} \quad g_i = T_B^* - T_B(R_1, R_2, C_{lw}, I_{ce}) \tag{8}$$

LMA is an iterative technique, like most other numerical minimization algorithms. The minimization starts with an initial guess for the parameter vector, p. In every iteration, p is replaced by a new estimate $(p + q)$. This is done as follows:

$$g(p + q) \approx g(p) + Jq \tag{9}$$

where J is a matrix of partial derivatives of g taken with respect to the parameters and is known as the Jacobian. The derivatives in many problems (including the present one) are numerically determined.

A minimum for S is being sought and so $\nabla S = 0$, leading to

$$(J^T J)q = -J^T g \tag{10}$$

q can be determined from the above equation by inverting $(J^T J)$. An important feature of the LMA is the use of a "damping" in Eq. (10), given by

$$(J^T J + \varepsilon)q = -J^T g \tag{11}$$

In Eq. (11), ε is a non-negative damping factor and can be increased or decreased depending on the reduction in S. The iterations stop when S reduces to a predefined limit (convergence criterion).

In this study, both, linear and nonlinear forms of regression equations were tried with the help of an option called "user defined model" in DATAFIT. The following final forms of the equations were chosen, based on the nature of the curves obtained from the sensitivity analysis and also by looking at the indices of the correlations obtained. Outside of these, the validity of the equations was also checked for different profiles which are not used for generating the regression equation.

4.2.1. Regression equations for frequencies 6.6 GHz and 10.7 GHz

$$\begin{aligned} T_B = {} & a_1 R_1 + a_2 C_{lw} + a_3 R_2 + a_4 I_{ce} + a_5 + a_6 R_1^2 \\ & + a_7 C_{lw}^2 + a_8 R_2^2 + a_9 I_{ce}^2 + a_{10} R_1 C_{lw} + a_{11} R_1 R_2 \\ & + a_{12} R_1 I_{ce} + a_{13} C_{lw} R_2 + a_{14} C_{lw} I_{ce} + a_{15} R_2 I_{ce} \end{aligned} \tag{12}$$

where for 6.6 GHz: $a_1 = 0.4065$; $a_2 = 0.1010$; $a_3 = 0.1832$; $a_4 = -0.0393$; $a_5 = 0.5181$; $a_6 = -0.0845$; $a_7 = -0.0108$; $a_8 = -0.0273$; $a_9 = -0.0279$; $a_{10} = -0.0806$; $a_{11} = -0.1304$; $a_{12} = -0.0229$; $a_{13} = -0.0185$; $a_{14} = -0.0005$; $a_{15} = 0.0085$; *for 10.7 GHz*: $a_1 = 0.7958$; $a_2 = 0.1710$; $a_3 = 0.1220$; $a_4 = -0.2425$; $a_5 = 0.5787$; $a_6 = -0.4351$; $a_7 = -0.0330$; $a_8 = -0.0375$; $a_9 = -0.0194$; $a_{10} = -0.2043$; $a_{11} = -0.1494$; $a_{12} = -0.0027$; $a_{13} = -0.0047$; $a_{14} = 0.0077$; $a_{15} = 0.0596$.

4.2.2. Regression equations for frequencies 19.35 GHz and 22.235 GHz

$$\begin{aligned} T_B = {} & a_1 + a_2 \ln(R_1) + a_3 C_{lw}^{a_{12}} + a_4 \ln(R_2) + a_5 \ln(I_{ce}) \\ & + a_6 R_1^{a_{11}} + a_7 R_2^{a_{10}} + a_8 I_{ce}^{a_9} \end{aligned} \tag{13}$$

where for 19.35 GHz: $a_1 = 1.17738$; $a_2 = 0.07525$; $a_3 = 0.04608$; $a_4 = 0.00247$; $a_5 = 0.00652$; $a_6 = -0.22653$; $a_7 = -0.09054$; $a_8 = -0.49170$; $a_9 = 0.61053$; $a_{10} = 0.66175$; $a_{11} = 0.42990$; $a_{12} = 0.32656$; *for 22.235 GHz*: $a_1 = 1.31005$; $a_2 = 0.06624$; $a_3 = 0.00035$; $a_4 = 0.00154$; $a_5 = 0.00387$; $a_6 = -0.36959$; $a_7 = -0.07465$; $a_8 = -0.39984$; $a_9 = 0.73184$; $a_{10} = 0.51273$; $a_{11} = 0.22472$; $a_{12} = -0.01636$.

4.2.3. Regression equations for frequencies 37.5 GHz and 85 GHz

$$\begin{aligned} T_B = {} & a_1 + a_2 \ln(R_1) + a_3 C_{lw} + a_4 \ln(R_2) + a_5 \ln(I_{ce}) \\ & + a_6 R_1 + a_7 R_2 + a_8 I_{ce}^{a_9} \end{aligned} \tag{14}$$

where for 37.5 GHz: $a_1 = 5.38629$; $a_2 = 0.01211$; $a_3 = -0.01892$; $a_4 = -0.01807$; $a_5 = 0.30366$; $a_6 = -0.06730$; $a_7 = 0.02924$; $a_8 = -5.14015$; $a_9 = 0.10625$; *for 85 GHz*: $a_1 = 0.07211$; $a_2 = -0.00243$; $a_3 = -0.01546$; $a_4 = -0.00447$; $a_5 = -0.13484$; $a_6 = -0.03928$; $a_7 = 0.02383$; $a_8 = 0.17900$; $a_9 = 1.25536$.

Plots that show the comparison between the actual brightness temperature (data set) and the brightness temperatures calculated using the above regression equations, for all the frequencies from 6.6 to 85 GHz, along with the indices of the correlations, are presented in Fig. 3.

A closer look at the above regression equations reveals several interesting features: (1) the presence of mixed or cross terms involving more than one variable denotes the complex interplay of the variables and (2) at higher frequencies both the rain rate and the ice content support a logarithmic relationship again signifying the nonlinearity, while the cloud liquid water content does not need a logarithmic term. The above discussion serves to prove that obtaining the forward regression equations (1) is not a routine mathematical exercise (2) involves considerable effort and tweaking and (3) is not trivial.

4.3. Inverse calculations using genetic algorithms

Here, the problem of concern is the retrieval of atmospheric constituents (Cloud Liquid Water Content, Rainfall Rate, and Ice Content) from the known brightness temperatures at different microwave frequencies. The problem can be solved by minimizing the objective function, which is again expressed as a sum of the square of the residuals between the calculated and known brightness temperature as follows:

$$f = \sum_{v_i=1}^{6} [T_B - T_B^*]_{v_i}^2 \tag{15}$$

In this study, the optimization is carried out using GA, as already mentioned. Since GA works with only maximization problems [30], as is expected of any evolutionary optimization technique, the objective function is modified as

$$F = 1 \Big/ \left(1 + \sum_{v_i=1}^{6} [T_B - T_B^*]_{v_i}^2\right) \tag{16}$$

GA is a robust parameter search technique based on the mechanics of natural genetics and natural selection. Unlike calculus-based methods, GA neither depends on the existence of derivatives nor on the initial values. Traditional optimization algorithms will converge to the minimum only if the objective function has only one broad minimum. Since the present objective function is nonlinear and multimodal, traditional optimization algorithms converge to a local minimum, which depends on the initial guess values. Results (not presented here) using a traditional optimization algorithm "sequential quadratic programming" confirmed that the final results depend on the initial guess and hence such algorithms are not suitable for the present problem. Thus, in this study, GA, which is very attractive and widely used for applications where the objective function is highly nonlinear and multimodal, is employed for the process of optimization. GA works iteration (generation) by iteration, successively generating and testing a population of strings. In the first generation, an initial population, which is a set of individuals (design parameters) each of which is represented in binary-coded strings, is randomly generated within the range of parameters. After evaluating the fitness of each individual, fitter individuals are selected for "reproducing" "offsprings" for the next generation. The selection process is determined by the objective function values. Some of the selected individuals are chosen to find mates and undergo the crossover operation, which is a reproduction process that makes offsprings by exchanging the "genes" of the "parents" to improve the fitness of the next generation. Then, some of the offsprings are chosen for the operation of "mutation" that preserves the diversity of a population. This is done by changing some of genes of the selected individual(s) within the range of design space and is done sparsely (typical mutation rates are less than 5%, i.e. if the solution space involves 1000 bits, less than 50 bits will be changed) and stochastically. Because there is no guarantee that GA will produce a monotonic improvement in the objective function value with variance of generation, due to its stochastic nature, an elitist strategy is used to ensure a monotonic improvement by copying the best individual of the present generation on to the next generation. Once the first generation is completed, the iterations will not stop until a satisfactory solution is reached. The highlights of the GA code used in the present study are (i) in the reproduction phase, fitter individuals are selected using tournament selection operator; (ii) uniform crossover operator, where cross over refers to exchange of bits between solutions similar to exchange of genetic information in reproduction is used; and (iii) instead of mutation, micro-GA is implemented. Details of the algorithm are explained with an example in Appendix A.

4.3.1. Solution procedure

The equations developed for the forward problem ((12)–(14)) using nonlinear regression analysis are used to obtain the brightness temperatures ($T_{B,v_{i=1--6}}$). T_B^* are the known brightness temperatures which are taken from the data set developed by solving the 6000 profiles that are not used for developing regression equations. T_B is a function of R_1, R_2, C_{lw}, I_{ce} and T_B^* is the known data. Hence, the objective function F is a function of only R_1, R_2, C_{lw} and I_{ce}. Therefore, R_1, R_2, C_{lw} and I_{ce} are the design parameters for the GA and all of these range from 0 to 1 (all parameters were normalized with respect to the respective maximum value). The constraints used to solve this problem along with Eq. (16) are

1. Variable constraint ($0 \leqslant (R_1, R_2, C_{lw}, I_{ce}) \leqslant 1$)
2. Inequality constraints

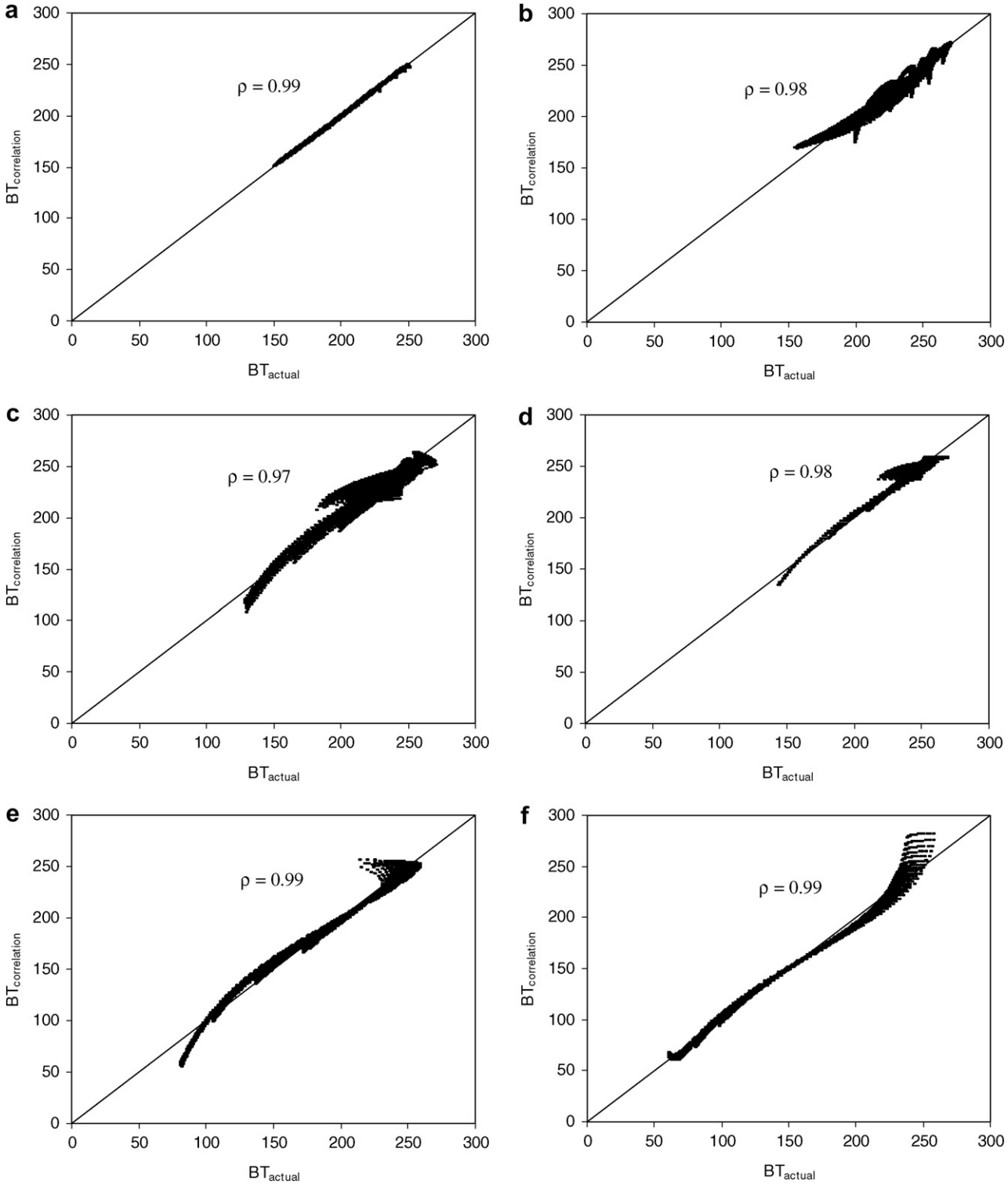

Fig. 3. Comparison between actual and correlated values of brightness temperature for different frequencies: (a) 6.6 GHz; (b) 10.7 GHz; (c) 19.35 GHz; (d) 22.235 GHz; (e) 37.5 GHz; and (f) 85 GHz.

(a) $0 \leqslant T_{\mathrm{B},v_{i=1--6}} \leqslant 1$;
(b) $R_2 < R_1$.

The variable constraints are taken care of while generating the population itself, such that all variables created will lie between 0 and 1. The inequality constraints are added to the objective function with a penalty parameter, such that if the constraint is violated, the penalty terms will become active. Inequality constraint 2b deserves special mention. It corresponds to the criterion that the rainfall in the 2nd layer cannot exceed that of the 1st layer – a thermodynamic necessity. The number of bits used to represent each vari-

able is taken as 10. The population size employed in this study is 14 and hence the GA will start by generating randomly 14 initial parameter sets of (R_1, R_2, C_{lw}, I_{ce}). For all these parameter sets, T_B is calculated for all the frequencies using (12)–(14). Using the objective function value, fitness is assigned to each parameter set. Using the fitness values, reproduction and crossover operators will determine the next 14 parameter sets of (R_1, R_2, C_{lw}, I_{ce}). The process repeats itself until a close enough fit is achieved. The maximum number of generations used is fixed at 250. The values of the number of bits, the population size and the number of generations indicated were determined by running a number of test cases with different combinations of these numbers. Those that gave better results in terms of computational economy and accuracy were finally selected.

5. Results

The parameters obtained through GA by using the brightness temperature values of the 6000 profiles which were not used for generating regression equations are plotted against the actual parameter values of the 6000 profiles and these are shown in the scatterogram (Fig. 4). A closer look at Fig. 4a shows that there is over prediction at low rainfall rates and underprediction at higher rainfall rates. Even so, the error band is within ±30% which is considered as acceptable in satellite meteorology. As far as Fig. 4b that corresponds to average rainfall rate is concerned, this bias is significantly reduced, though the error band remains the same. From both the figures, it can be observed that, as expected, the predictions get worse at lower rainfall rates, where the scattering is not so strong. From Fig. 4d, it is seen that the retrieval of ice content is very good with very little scatter. Furthermore, as expected, due to the nature of the problem where cloud liquid water has negligible influence over brightness temperature in the presence of rain and ice, it is not possible to estimate the cloud liquid water content (the large scatter is seen in Fig. 4c), where as the other parameters such as precipitation (1st layer rainfall rate), cumulative rainfall rate and cumulative ice content

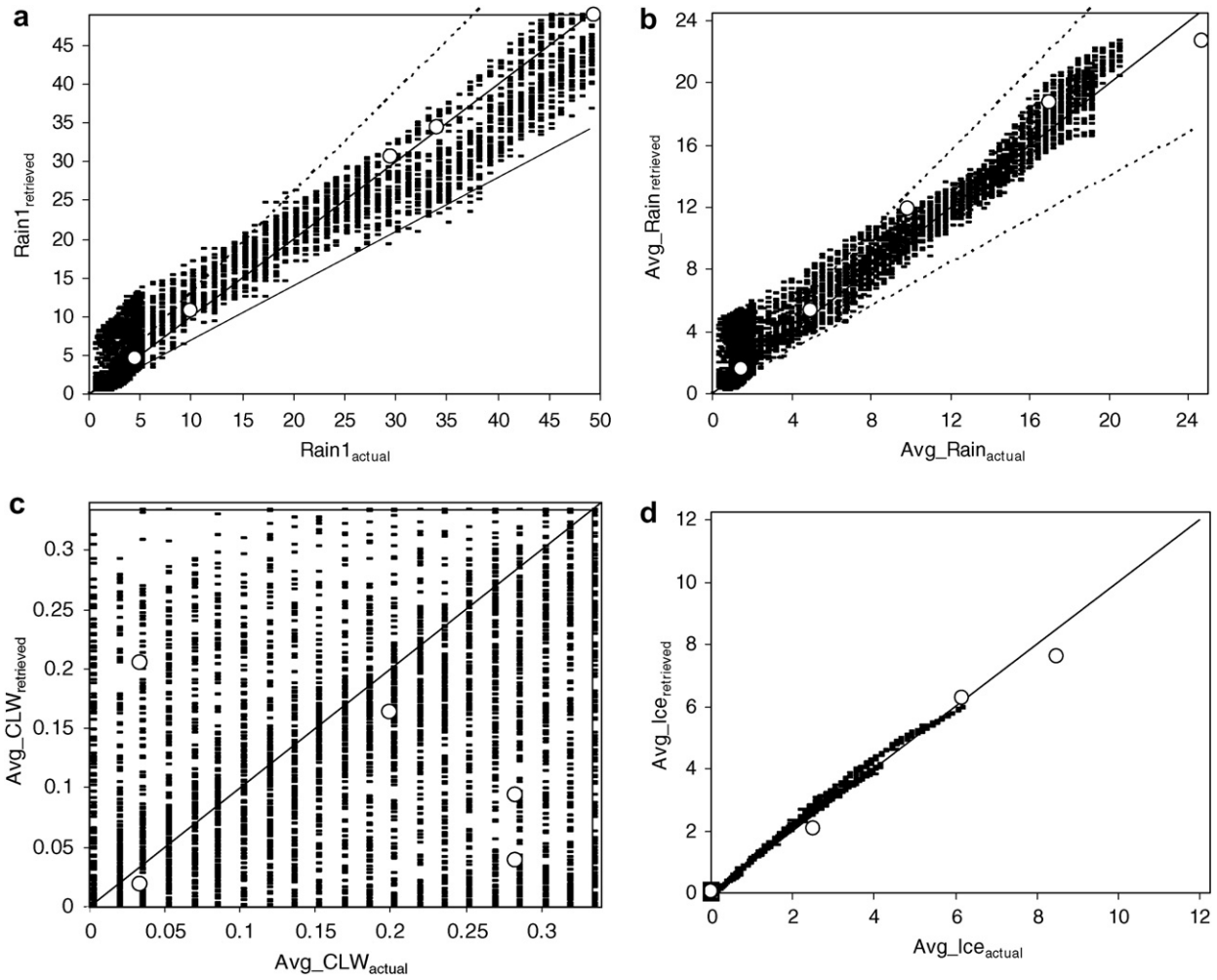

Fig. 4. Comparison between actual values and estimated values using genetic algorithms for 6000 profiles which were not used for developing correlations. The error band in (a) and (b) is ±30%. Symbol ○ represents parameters retrieved by using direct formulation repeatedly instead of using regression equations.

are satisfactorily estimated. The error in the retrieval of parameters is not due to the retrieval algorithm used *per se* but is because of (1) the nature of the problem and (2) the error present in the forward regression equations.

The results of inverse problem for five different atmospheric profiles, in which optimization is carried out by running the direct problem repeatedly instead of using regression equations are also plotted in Fig. 4 and these are represented using white circles (see Swaminathan [31] for a fuller discussion on the inverse regression analysis approach). Even though the results turn out to be good, the time consumed for solving each profile is very high in comparison and makes this method impossible for practical purposes. By running the direct problem repeatedly instead of using regression equations, the time consumed for retrieving parameters from a single profile roughly varies between 90 and 120 min on a 1 GB RAM, Pentium 4 processor, whereas, for the case of using regression equations along with GA, it takes only 9.6 min for retrieving the parameters from a set of 6000 profiles on a computer with the same configuration. If better regression equations are developed for the forward problem and used in the retrieval, then the error in the parameter estimation is expected to decrease. Future studies in the direction of improving forward regression models, hopefully may be able to decrease the errors associated with full blown retrievals.

6. Conclusions

In this study, a new hybrid regression/genetic algorithm method for the retrieval of hydrometeors from microwave radiances has been proposed. A finite volume method is used to solve the forward problem that employs a three layered model for the precipitating atmosphere, to determine the top of the atmosphere radiances. These radiances are used in the retrieval algorithms to minimize the error with respect to the satellite measured radiances. A sensitivity analysis using synthetic profiles of atmosphere and a trend analysis that elucidates the hidden physical insight are presented. A hybrid method has been developed to estimate the atmospheric constituents. This combines regression analysis for the brightness temperatures for six different microwave frequencies from the known atmospheric profiles for the forward problem with GA for the inverse problem. Forward regression analysis, along with inverse analysis using GA, estimates the precipitable rainfall rate and column average rainfall rate to within ±30% of the actual data and the estimated ice content represents the actual data very well. The results show that the presence of cloud liquid water content has negligible influence over the brightness temperature in the presence of rain and ice. Hence, the retrieval of cloud liquid content is not possible in the presence of other constituents when radiative transfer models that include scattering are made use of.

In this work, the focus was on developing a fast and efficient technique for the "simultaneous" retrieval of hydrometeors. The technique involves the use of contemporary optimization techniques for both the forward and the inverse problems. In order to keep the problem tractable, the number of parameters to be retrieved was kept small, by design. This necessitated the use of a simple model for the precipitating atmosphere. Even so, extension to situations involving simultaneous retrieval of more number of parameters with a more complex atmosphere model is completely feasible within the framework presented in the paper.

Appendix A. Genetic algorithms through an example

Consider the problem that was solved in Section 4.3. In what follows, the basic GA operators: Reproduction, crossover and micro-GA are detailed out. As the constraints would not play a role in the demonstration of the three operators in GA, they are ignored.

The objective function without constraints is

$$F = \frac{1}{\left(1 + \sum_{v_i=1}^{6} (T_B - T_B^*)_{v_i}^2\right)} \tag{17}$$

T_B's are calculated using Eqs. (12)–(14).
F is a function of (R_1, C_{lw}, R_2, I_{ce}).

A.1. Input For GA

- Let the known values of T_B^* (normalized) be (0.8100, 0.8128, 0.2684, 0.6645, 0.3923, 0.2458) corresponding to the frequencies (6.600, 10.700, 19.350, 22.235, 35.500, 85.000) in GHz, respectively.
- Since F is a function of four variables (R_1, C_{lw}, R_2, I_{ce}); Number of parameters = 4 and let these be denoted by X_1, X_2, X_3, X_4.
- String length (Number of bits used to represent each variable) = 10.
- Population size = 14.
- Since all the variables are normalized, the upper and lower limit for each variable can be taken as $0.001 \leqslant X_i \leqslant 1.0$; where $i = 1, 2, 3, 4$.
- Total number of generations equivalent to the number of iteration in a numerical solution is taken as 250.

A.2. Steps involved in GA

GA works iteration (generation) by iteration. Here, the steps involved in a single generation are explained.

An initial population, which is a set of individuals (design parameters), each of which is represented by a binary-coded string, is randomly generated within the range of parameters as shown in Table A.1.

The number of zeros in the above Table is 277 and the number of ones is 283 and can be considered as confirming that the random number generation is random.

Table A.1
Initial population set in a binary code representation

#	Binary code			
	X_1	X_2	X_3	X_4
1	1110101011	0011101111	0111100111	0001110101
2	0101010010	0001011000	0100110010	1100000110
3	1110110010	1001100101	0001100100	1100111000
4	0011000111	1000011111	0111100110	0000010001
5	1101000100	0110001010	0011100110	1101101100
6	1100001100	1100100000	0001101010	0001011111
7	1111000010	0110011111	0001011111	1001001110
8	1000101001	1010110101	1001110011	1000101111
9	1000111101	1001100101	1100000000	1101100101
10	1001011001	1011010001	1011110000	0111100100
11	1111010000	0100011100	0010100010	1100001000
12	1000110111	1011101100	1101010101	1110000101
13	0110011100	1011111110	0000011111	0001111010
14	0110001100	1101000111	0111010100	0111101111

The binary-coded strings are decoded to obtain the actual values as

$$X_i = X_i^{(\mathrm{L})} + \frac{X_i^{(\mathrm{U})} - X_i^{(\mathrm{L})}}{2^{l_i} - 1} \quad \text{decoded value } (X_i) \tag{18}$$

For example, consider the first entry in Table A.1

$$X_{(1110101011)} = 0.001 + \frac{1 - 0.001}{2^{10} - 1} * 939 = 0.9180$$

The actual values are shown in Table A.2.

For each parameter set, the objective function value is calculated with the regression equations developed earlier (Eqs. (12)–(14)) to assign fitness (Eq. (17)). Here, the value of objective function itself is taken as the fitness value and the fitness values for the initial population are shown in Table A.3.

A.2.1. Reproduction

Selects good strings in the population and forms a mating pool. Here, tournament selection is used.

Tournament selection is based on the general rule that is followed in any tournament. In a cricket or tennis tournament for example, to select one, two teams will play and the winner will be selected. This continues till all the winners are selected. Here too, the same method is followed and hence it is called tournament selection. The process of selecting the mating pool from the given population is shown in Table A.3.

Table A.2
Actual values of the initial population set

#	Actual values			
	X_1	X_2	X_3	X_4
1	0.9180	0.2344	0.4766	0.1153
2	0.3311	0.0869	0.2998	0.7568
3	0.9248	0.5996	0.0987	0.8057
4	0.1953	0.5313	0.4756	0.0176
5	0.8174	0.3858	0.2256	0.8564
6	0.7627	0.7822	0.1045	0.0938
7	0.9404	0.4063	0.0938	0.5772
8	0.5410	0.6777	0.6133	0.5469
9	0.5606	0.5996	0.7510	0.8496
10	0.5879	0.7051	0.7354	0.4736
11	0.9541	0.2783	0.1592	0.7588
12	0.5547	0.7315	0.8340	0.8809
13	0.4033	0.7490	0.0313	0.1201
14	0.3877	0.8203	0.4580	0.4844

Table A.3
Mating pool selection using fitness values

#	Binary code				Fitness	Mating pool
	X_1	X_2	X_3	X_4		
1	1110101011	0011101111	0111100111	0001110101	0.90221	
2	0101010010	0001011000	0100110010	1100000110	0.92212	←
3	1110110010	1001100101	0001100100	1100111000	0.95871	←
4	0011000111	1000011111	0111100110	0000010001	0.71157	
5	1101000100	0110001010	0011100110	1101101100	0.94481	←
6	1100001100	1100100000	0001101010	0001011111	0.85619	
7	1111000010	0110011111	0001011111	1001001110	0.9946	←
8	1000101001	1010110101	1001110011	1000101111	0.99352	
9	1000111101	1001100101	1100000000	1101100101	0.9368	
10	1001011001	1011010001	1011110000	0111100100	0.99847	←
11	1111010000	0100011100	0010100010	1100001000	0.96692	←
12	1000110111	1011101100	1101010101	1110000101	0.92817	
13	0110011100	1011111110	0000011111	0001111010	0.85718	
14	0110001100	1101000111	0111010100	0111101111	0.99291	←

The average fitness of the population in Table A.3 is 0.926, with the maximum fitness being 0.9984 and the minimum fitness being 0.7116.

As shown in the Table A.3, out of first two parameter sets, the one that has higher fitness value is selected for the mating pool (shown by an leftward pointing arrow mark). Similarly out of the next two, the one that has higher fitness value is selected for the mating pool and the process continues till sufficient entries are available in the mating pool that can produce a new population set equal to that of current one. In the current procedure, the mating pool should have entries equal to that of original population. Hence, from the above Table, it is possible to get only half of the number of population in the mating pool. In order to get the other members in the mating pool, the initial population set is shuffled randomly and again the process continues to select the remaining parameter set to complete the selection procedure for the mating pool. In the process good strings (high fitness value) will have large number of copies. The mating pool is shown in Table A.4.

Table A.4
Mating pool with pairs of parents ready for crossover operator

#	Mating pool				Parent
	X_1	X_2	X_3	X_4	
1	0101010010	0001011000	0100110010	1100000110	1
2	1110110010	1001100101	0001100100	1100111000	2
3	1101000100	0110001010	0011100110	1101101100	1
4	1111000010	0110011111	0001011111	1001001110	2
⋮	⋮	⋮	⋮	⋮	⋮
⋮	⋮	⋮	⋮	⋮	⋮

Table A.5
Crossover operation for a single parameter

	Parent (X_1)										Child (X_1) after "crossover"									
1	0	1	0	1	0	1	0	0	1	0	1	1	1	1	0	1	0	0	1	0
2	1	1	1	0	1	1	0	0	1	0	0	1	0	0	1	1	0	0	1	0
Random number	0.7	0.1	0.9	0.0	0.3	0.5	0.2	0.8	0.6	0.4										
Exchange bit	Y	N	Y	N	N	N	N	Y	Y	N										

A.2.2. Crossover

In the mating pool, the first two parameter sets form one pair of parents (Table A.4) that will be involved in the next set of operations to produce two parameter sets (called child), by exchanging information among themselves. This process is called crossover. There are different crossover operators available. In this study, uniform crossover is used. In this type of crossover, for each bit, the decision to exchange the bits between the parents is made depending on the probability of crossover. The process of crossover for a parameter from the parent to child is shown in Table A.5 for a probability of crossover equal to 0.5.

The process of selection to decide whether to exchange the bits between the parents is carried out using a random number generator and the random number generator is allowed to generate numbers between 0 and 1. Since the probability of cross over is fixed as 0.5, if the random number turns out to be greater than 0.5, the corresponding bits are exchanged (in Table A.5 "Y" indicates yes and "N" indicates no to exchange of bits).

A.2.3. Micro-GA

Here, the bits of the best fitness parameter set are compared with corresponding bits of all other parameter sets, and if the number of bits which are different from the best parameter set are less than 5% of total number of bits present in the total population, then the algorithm considers the population as converged and retains only the best fitness parameter set and replaces all other parameter sets with a new parameter set created, randomly as was done in the first step. Hence, the micro-GA implementation will not occur in every generation, but only if this condition arises.

The above steps constitute one generation and will repeat till convergence. In the present study, the number of generations is fixed at 250, based on experience gained by repeating the process for several test cases.

At the end of the 250 generations, the set of parameters obtained are shown in Table A.6.

The average fitness of the final population is 0.99959 with the maximum and minimum fitness varying by just 2.4×10^{-4}. With GA not only have we achieved convergence, but the variation of fitness or quality within the population is also significantly reduced.

Table A.6
Final parameter set at the end of 250 generations

#	Binary code				Fitness
	X_1	X_2	X_3	X_4	
1	1011010011	1110101100	1111111111	0110101000	0.99963
2	1011010011	1110110100	1111110111	0110101000	0.99963
3	1011011011	1110100010	1111110111	0110101000	0.99963
4	1011010011	1110101000	1111111111	0110101000	0.99963
5	1011010011	1110100100	1111111111	0110101000	0.99963
6	1011010001	1110100010	1111111111	0110101000	0.99963
7	1011010111	0110111000	1111111111	0110101000	0.99941
8	1011010011	1110100100	1111111111	0110101000	0.99963
9	1011010011	1110100010	1111110111	0110101000	0.99963
10	1011010001	1110100010	1111110111	0110101000	0.99963
11	1011011011	1111110000	1111111110	0110101000	0.99961
12	1011010011	1110100000	1111111111	0110101000	0.99963
13	1001010011	1110101100	1111111111	0110101000	0.99939
14	1011110011	1110100000	1111110111	0110101000	0.99960

References

[1] E.A. Smith, J.E. Lamm, R. Adler, J. Alishouse, K. Aonashi, E. Barrett, P. Bauer, W. Berg, A. Chang, R. Ferraro, J. Ferriday, S. Goodman, N. Grody, C. Kidd, D. Kniveton, C. Kummerow, G. Liu, F. Marzano, A. Mugnai, W. Olson, G. Petty, A. Shibata, R. Specer, F. Wentz, T. Wilheit, E. Zipser, Results of the WetNet PIP-2 Project, J. Atmos. Sci. 55 (1998) 1483–1536.

[2] W.B. Rossow, R.A. Schiffer, ISCCP cloud data products, Bull. Am. Meteorol. Soc. 72 (1991) 2–20.

[3] R.F. Adler, C. Kidd, G. Petty, M. Morrissey, H.M. Goodman, Intercomparison of global precipitation products: the third precipitation intercomparison Project (PIP-3), Bull. Am. Meteorol. Soc. 82 (7) (2001) 1377–1396.

[4] P. Bauer, J.P.V. Poiares Baptista, M. de Iulis, The effect of the melting layer on the microwave emission of clouds over the ocean, J. Atmos. Sci. 56 (6) (1999) 852–867.

[5] C. Kummerow, Beamfilling errors in passive microwave rainfall retrievals, J. Appl. Meteorol. 37 (4) (1998) 356–370.

[6] G. Panegrossi, S. Dietrich, F.S. Marzano, A. Mugnai, E.A. Smith, X. Xiang, J. Tripoli, P.K. Wang, J.P.V. Poiares Baptista, Use of cloud model microphysics for passive microwave-based precipitation retrieval: significance of consistency between model and measurement manifolds, J. Atmos. Sci. 55 (9) (1998) 1644–1673.

[7] G.W. Petty, K.B. Katsaros, The response of the SSM/I to the marine environment. Part II: a parameterization of the effect of the sea surface slope distribution on emission and reflection, J. Atmos. Ocean. Technol. 11 (3) (1994) 617–628.

[8] T. Wilheit, C.D. Kummerow, R. Ferraro, Rainfall algorithms for AMSR-E, IEEE Trans. Geosci. Remote Sensing 41 (2) (2003) 204–213.

[9] J. Ikai, K. Nakamura, Comparison of rain rates over the ocean derived from TRMM Microwave Imager and Precipitation Radar, J. Atmos. Ocean. Technol. 20 (2003) 1709–1726.

[10] C. Kummerow, W.S. Olson, L. Giglio, A simplified scheme for obtaining precipitation and vertical hydrometeor profiles from passive microwave sensors, IEEE Trans. Geosci. Remote Sensing 34 (5) (1996) 1213–1232.

[11] T.T. Wilheit, A.T.C. Chang, M.S.V. Rao, E.B. Rodgers, J.S. Theon, A satellite technique for quantitatively mapping rainfall rates over the oceans, J. Appl. Meteorol. 16 (5) (1977) 551–560.
[12] R.W. Spencer, A satellite passive 37-GHz scattering-based method for measuring oceanic rain rates, J. Clim. Appl. Meteorol. 25 (6) (1986) 754–766.
[13] C. Kummerow, L. Giglio, A passive microwave technique for estimating rainfall and vertical structure information from space. Part I: algorithm description, J. Appl. Meteorol. 33 (1994) 3–18.
[14] A.T.C. Chang, L.S. Chiu, C. Kummerow, J. Meng, T.T. Wilheit, First results of the TRMM Microwave Imager (TMI) monthly oceanic rain rate: comparison with SSM/I, Geophys. Res. Lett. 26 (1999) 2379–2382.
[15] K. Krishnakumar, Micro-genetic algorithms for stationary and non-stationary function optimization, *intelligent control and adaptive systems*, SPIE 1196 (1989) 289–296.
[16] G. Syswerda, Uniform crossover in genetic algorithms, in: J. Schaffer (Ed.), Proceedings of the Third International Conference on Genetic Algorithms, Morgan Kaufmann Publishers, Los Altos, CA, 1989, pp. 2–9.
[17] D.L. Carroll, Genetic algorithms and optimizing chemical oxygen–iodine lasers, in: H.B. Wilson, R.C. Batra, C.W. Bert, A.M.J. Davis, R.A. Schapery, D.S. Stewart, F.F. Swinson (Eds.), Developments in Theoretical and Applied Mechanics, vol. XVIII, School of Engineering, The University of Alabama, 1996, pp. 411–424.
[18] G. Liu, J.A. Curry, Retrieval of precipitation from satellite microwave measurements using both emission and scattering, J. Geophys. Res. 97 (1992) 9959–9974.
[19] J.G. Ferriday, S.K. Avery, Passive microwave remote sensing of rainfall with SSM/I: algorithm development and implementation, J. Appl. Meteorol. 33 (1994) 1587–1596.
[20] B. Lin, P. Minnis, Temporal variations of land surface microwave emissivities over the atmospheric radiation measurement program southern great plains site, J. Appl. Meteorol. 39 (2000) 1103–1116.
[21] R. Siegel, J.R. Howell, Thermal Radiation Heat Transfer, third ed., Taylor and Francis, Washington, 1992, 1072pp.
[22] J.B. Buglia, Introduction to the theory of atmospheric radiative transfer, NASA Reference Publication 1156 (1986) 175.
[23] G.D. Raithby, E.H. Chui, A Finite-Volume method for predicting radiant heat transfer in enclosures with participating media, J. Heat Transfer 112 (1990) 415–423.
[24] V. Swaminathan, C. Balaji, S.P. Venkateshan, Parameter estimation in two-layer planar gray participating medium, J. Thermophys Heat Transfer 18 (2004) 187–192.
[25] V. Swaminathan, R.M. Gairola, C. Balaji, S.P. Venkateshan, Estimation of microwave radiation intensity from a multi-layered cloud model, J. Thermophys. Heat Transfer 19 (2005) 343–352.
[26] F.M. Modest, Radiative Heat Transfer, second ed., Academic Press, California, 2003, 822pp.
[27] C. Kummerow, On the accuracy of the Eddington approximation for radiative transfer in the microwave frequencies, J. Geophys. Res. 98 (1993) 2757–2765.
[28] M.S. Tatarskaia, R.J. Lataitis, B.A. Stankov, V.V. Tatarskii, A numerical method for synthesizing atmospheric temperature and humidity profiles, J. Appl. Meteorol. 37 (1998) 718–729.
[29] Datafit 8.1 Documentation Guide, Oakdale Engineering, Pasadena, 2006.
[30] Kalyanmoy Deb, Optimization for Engineering Design, second ed., Prentice-Hall, India, 1995, 381pp.
[31] V. Swaminathan, Inverse Radiation Problems in Participating Media, Ph.D Thesis, Department of Mechanical Engineering, Indian Institute of Technology, Madras, India, March, 2005.